# Synchronous In Situ ATPase Activity, Mechanics, and $Ca^{2+}$ Sensitivity of Human and Porcine Myocardium

P. J. Griffiths,[†*] H. Isackson,[‡] R. Pelc,[§] C. S. Redwood,[‡] S. S. Funari,[¶] H. Watkins,[‡] and C. C. Ashley[†]
[†]Department of Physiology, Anatomy and Genetics, University of Oxford, Oxford, United Kingdom; [‡]Department of Cardiovascular Medicine, John Radcliffe Hospital, Oxford, United Kingdom; [§]Institute of Physiology, Academy of Sciences, Vídenská, Prague, Czech Republic; and [¶]Hasylab at DESY, Deutsches Elektronen Synchrotron, Hamburg, Germany

ABSTRACT Flash-frozen myocardium samples provide a valuable means of correlating clinical cardiomyopathies with abnormalities in sarcomeric contractile and biochemical parameters. We examined flash-frozen left-ventricle human cardiomyocyte bundles from healthy donors to determine control parameters for isometric tension ($P_o$) development and $Ca^{2+}$ sensitivity, while simultaneously measuring actomyosin ATPase activity in situ by a fluorimetric technique. $P_o$ was 17 kN $m^{-2}$ and $pCa_{50\%}$ was 5.99 (28°C, $I = 130$ mM). ATPase activity increased linearly with tension to 132 $\mu$M $s^{-1}$. To determine the influence of flash-freezing, we compared the same parameters in both glycerinated and flash-frozen porcine left-ventricle trabeculae. $P_o$ in glycerinated porcine myocardium was 25 kN $m^{-2}$, and maximum ATPase activity was 183 $\mu$M $s^{-1}$. In flash-frozen porcine myocardium, $P_o$ was 16 kN $m^{-2}$ and maximum ATPase activity was 207 $\mu$M $s^{-1}$. $pCa_{50\%}$ was 5.77 in the glycerinated and 5.83 in the flash-frozen sample. Both passive and active stiffness of flash-frozen porcine myocardium were lower than for glycerinated tissue and similar to the human samples. Although lower stiffness and isometric tension development may indicate flash-freezing impairment of axial force transmission, we cannot exclude variability between samples as the cause. ATPase activity and $pCa_{50\%}$ were unaffected by flash-freezing. The lower ATPase activity measured in human tissue suggests a slower actomyosin turnover by the contractile proteins.

## INTRODUCTION

Intrinsic cardiomyopathies result from inherent myocardial defects, as distinct from extrinsic cardiomyopathies, which are caused by external agents. Many intrinsic cardiomyopathies have been linked to mutations in essential sarcomeric proteins causing malfunction of cellular physiological processes. One approach to studying the physiological effects of these mutations is by protein exchange onto (or extraction from) an animal template (1–3), but the exchange or extraction procedure may affect physiological performance, and these techniques cannot reveal possible compensatory changes in other sarcomeric processes caused by mutant-induced impairment of myocyte function. Transgenic animal studies are not subject to these complications, but are not feasible for human tissue. Instead, cardiomyectomy samples from cardiomyopathic patients with known mutations of sarcomeric proteins provide an alternative approach, allowing clinical and hemodynamic pathology to be better matched with cellular and molecular myocardial abnormalities. To examine the functional consequences of specific mutations in human myocardium, we first determined these parameters for control flash-frozen myectomy samples from healthy donors showing no evidence of irregularities in cardiac performance.

Our human myectomy samples were flash-frozen in liquid nitrogen (77.2 K) and stored in solid $CO_2$ at 193 K (cryopreservation), as compared to the more conventional method of glycerination for striated muscle storage, where tissue is first loaded with a buffered 50% glycerol solution, then stored at −20 to −25°C (slightly above the freezing point of the glycerol mixture). Glycerol prevents ice crystal formation, which can disrupt cellular structure, damage membrane systems, and impair physiological performance. Optimal cryopreservation, by either flash-freezing (4) or slow cooling in the presence of a cryoprotectant (5), produces vitrification, a noncrystalline, amorphous solidification of the sarcoplasm that is a less deleterious process than ice crystallization (6). However, flash-freezing in liquid nitrogen causes a gaseous layer to form between the tissue and the liquid nitrogen, which acts as an insulator and significantly slows the freezing process (the Leidenfrost effect), enabling ice crystal growth instead of vitrification and restricting the vitrified region to just a few microns in depth. Nevertheless, skinned myocytes from flash-frozen human myocardium have been used successfully to determine calcium sensitivity and contractile force (7) and ATPase activity (8), and they show no pronounced differences from fresh tissue in sarcomere regularity or calcium sensitivity (9). To detect any influence from the Leidenfrost effect on myocardial parameters, we examined the same parameters in porcine myocardium that had been either flash-frozen or preserved by conventional glycerination. Pig heart resembles the human heart in size, anatomy, and function, so porcine myocardium would be expected to show similarities to human tissue in its regulation of activation and its force-generating efficiency.

The properties we examined were $Ca^{2+}$ sensitivity, isometric force generation, stiffness, and ATPase activity.

*Submitted April 1, 2009, and accepted for publication July 23, 2009.*

*Correspondence: pjg@dpag.ox.ac.uk

Editor: K. W. Ranatunga.



0006-3495/09/11/2503/10 $2.00

doi: 10.1016/j.bpj.2009.07.058

Previous studies of actomyosin ATPase activity in porcine and human myocardium used either extracted S1 moieties of myosin for in vitro assay or measurement of ADP production in the bathing medium during activation of skinned cardiac preparations (10–12). ATPase activity measurements from myosin in solution lack the constraints imposed on the cross-bridge cycle by the lattice structure of the contractile proteins and by the absence of load on the actomyosin intermediates of the cycle, whereas cuvette measurements of ADP production from skinned cells require an estimate of the tissue volume to calculate ATPase activity, are subject to errors in solution transfers, and are unsuitable for time-resolved studies of changes in ATP turnover rate. Griffiths et al. (13) developed an enzyme-linked fluorimetric assay method for frog skeletal muscle fibers in which time-resolved ATPase activity and force were measured simultaneously during contraction. Subsequently, this approach has been applied successfully in rat and toad skeletal muscle (14) and in rabbit psoas (15). Here, we report a version of this method that permits an in situ study of ATPase activity in cardiac muscle, making use of advances in modern semiconductor technology to simplify and improve the measurements.

## METHODS

### Preparations

Human tissue samples were obtained from Prof. C. Dos Remedios (University of Sydney, Sydney, Australia) via Prof. S. Marston (Imperial College, London). Ethical approval was obtained from St. Vincent's Hospital, Sydney, and the investigation conformed to the principles outlined in the Declaration of Helsinki. Samples of left-ventricular muscle were obtained from adult donor hearts for which no suitable transplant recipient had been found and were immediately frozen in liquid nitrogen and maintained at 193 K until use. The samples have been previously described by Messer et al. (16). Details of the dissection and preparation of samples are provided in section S.1 of the Supporting Material.

### Solutions

Stock solution composition was (in mM) $Na_2ATP$, 5; EGTA, 5; imidazole, 20; $Mg(OH)_2$, 5.6; potassium propionate, 10; pH 7.0 at 23°C. For Ca-activating solutions, 5 mM $CaCl_2$ was added and KOH replaced potassium propionate. For ATPase measurements, 10–15 mM phosphoenol pyruvate (PEP) was added, the solution pH was titrated to 7.0 with KOH, then 10–12 mM reduced nicotinamide adenine dinucleotide (NADH) and 500 units/ml pyruvate kinase (PK) and lactate dehydrogenase (LDH) were added (ionic strength of ATPase solutions, 130 mM). For other purposes, potassium propionate was added to replace the ionic strength contribution of PEP and NADH, with a further 1% Triton X100 for preparation of "skinning" solutions. Free $[Ca^{2+}]$ was calculated for mixtures of activating and relaxing solutions using a modified form of the method of Perrin and Sayce (17) and checked by using a calcium electrode (Orion 97-20 Ionplus, Thermo Electron, Witchford, United Kingdom).

### Experimental setup

Cardiac muscle strips were attached between stainless steel pins projecting from a force transducer (AE 801, sensitivity 0.44 mV $\mu N^{-1}$, resonance frequency 8 kHz; HJK Sensoren und Systeme Verwaltungs, Friedberg, Germany) and a moving coil motor (step time, 180 $\mu$s) using cyanoacrylate adhesive. The adhesive was mixed with finely powdered carbon to permit measurement of the precise length of glue-free tissue and to ensure that the ends and circumference of the strip were fixed at the point of contact with the pins. It also removed any fluorescence arising from the adhesive itself. The strip was then immersed in relaxing solution contained in 80-$\mu$l glass-walled chambers mounted in a solution-changing device (18,19) capable of exchanging solutions within 500 ms. Sarcomere length was determined by laser diffraction, using a diode laser beam ($\lambda = 670$ nm) illuminating a 0.7-mm segment of the strip. For further details, see section S.2 of the Supporting Material, and Fig. S1.

### ATPase activity measurement in skinned cardiac muscle

We used the enzyme-linked assay system shown below:

$$\mathrm{PEP} + \mathrm{ADP} + \mathrm{H^+} \xrightarrow{\text{pyruvate kinase}} \text{pyruvate} + \mathrm{ATP} \quad (1)$$

$$\text{pyruvate} + \mathrm{NADH} + \mathrm{H^+} \xrightleftharpoons{\text{loctate dehydrogenase}} \text{lactate} + \mathrm{NAD^+} \quad (2)$$

The equilibrium of reaction 1 lies strongly to the right under the conditions of the assay ($K' = [\text{pyruvate}][\text{ATP}]/[\text{PEP}][\text{ADP}] = 3.89 \times 10^4$, where each reactant represents the sum of all the ionic and metal-complexed species; pH 7.0, 1.0 mM $[Mg^{2+}]$, ionic strength = 0.25 M, 25°C (20)); reaction 2 is an equilibrium reaction ($K' = [\text{lactate}][NAD^+]/[\text{pyruvate}][\text{NADH}] = 3.6 \times 10^4$ at pH 7.0, 25°C) that favors NADH consumption. The overall reaction is a replenishment of ATP at the expense of NADH and PEP. To ensure that ATP regeneration is fast enough to cope with ATP hydrolysis, we used sufficiently high concentrations of enzymes (500 U/ml) that enzyme levels were not rate-limiting in the ATPase measurements.

### Radial diffusion coefficient estimation

We measured the rate of loading of preparations with either NADH or fluorescent dextran (molecular mass 155 kDa). The loading data were fitted to a model of diffusion in a muscle segment of either cylindrical or rectangular cross section using a Levenberg-Marquardt least-squares regression and an adaptive step size Runge-Kutta method (21) to obtain the best-fit value of the radial diffusion coefficient ($D$). Details are provided in section S.3 of the Supporting Material.

### Experimental protocol

Strips were incubated for 30 min in the ATPase assay system to permit enzyme diffusion into the preparation. Longer incubations (up to 24 h) produced no discernible change in the efficacy of the assay. Sarcomere length was adjusted to 2.15–2.30 $\mu$m, the long end of the cardiac working range, chosen to maximize force and ATPase activity, although ATPase activity is much less sensitive to sarcomere length than is force (22). At these lengths, a small resting tension was present in the relaxed state. It could be seen, using electron microscopy of flash-frozen porcine tissue, that tissue structure was well preserved in cryopreserved myocardium (see section S.4 in the Supporting Material). We used an automatic timing system to control data collection, solution changes, and UV illumination. At time zero, the preparation was transferred to a washing chamber (relaxing solution without NADH) for 240 ms, and then to a measuring chamber containing light-grade liquid paraffin (BDH, Poole, United Kingdom) for 60 s, during which time it was exposed to UV radiation ($\lambda = 365$ nm). Immediately after the measurement, the preparation was relaxed, UV illumination was terminated, and 10 s of background intensity was measured. At the start of the experiment, we measured autofluorescence in relaxing solution without NADH. We then calibrated the fluorescence signal by loading the preparation for 5 min with a known NADH concentration ([NADH]), with

zero PEP. The difference between calibration and autofluorescence was taken as the fluorescence signal of that [NADH] in the preparation ($\Delta F$). We then measured fluorescence at different levels of activation in our ATPase assay solutions. Except when the substrate supply was close to exhaustion, NADH fluorescence declined linearly with time, so we used linear-regression curve fitting to obtain the slope of the fluorescence decrease ($dF/dt$), and obtained ATPase activity as

$$d[\mathrm{ATP}]/dt = \frac{dF/dt}{\Delta F}[\mathrm{NADH}]. \quad (3)$$

Fluorescence intensity at >600 nm increased during NADH consumption because of the decreasing NADH absorbance at 365 nm as a result of NADH oxidation. No corrections for source intensity were required. Unless otherwise stated, all experiments were performed at 28°C. At the end of the experiment, the preparation was removed from the experimental chambers, and its length and diameter in both the vertical and horizontal planes were recorded.

Errors in parameters and error bars in figures are standard errors.

## RESULTS

### Porcine myocardium

Calcium sensitivity was determined from force developed in ATPase assay solutions of differing pCa after stabilization (typically 2–3 min) and minus resting tension. Maximum force ($P_o$) was measured throughout the experiment to check tissue condition. In most preparations, no decline in $P_o$ was evident over a period of several hours. In contrast, there was a noticeable shift in calcium sensitivity toward lower pCa values during long experiments. Active force development was fitted to the equation

$$\frac{P}{P_o} = \frac{K^q[\mathrm{Ca}^{2+}]^q}{1 + K^q[\mathrm{Ca}^{2+}]^q}. \quad (4)$$

using a Levenberg-Marquardt algorithm (21) to obtain calcium sensitivity. The value of $K$ in glycerinated porcine myocardium was $5.87 \pm 1.29 \times 10^5\ \mathrm{M}^{-1}$ (pK 5.77, $n = 13$), with a slope ($q$) of 1.02 (Fig. 1 *A*). Typically, $q$ is 2–3 for cardiac muscle, so to determine whether our experimental conditions had affected $q$, in five porcine preparations we used creatine phosphate/kinase (CrP/K) to replace lactate dehydrogenase/pyruvate kinase/PEP (LDH/PK). To balance ionic strength for PEP replacement by CrP, we added 60 mM potassium propionate to solutions; the composition was otherwise unaltered. The fitted parameters for the pCa curve with CrP/K were $K = 2.63 \pm 0.81 \times 10^5\ \mathrm{M}^{-1}$ (pK 5.42) and $q = 0.93$, indicating that selection of the CrP/K ATP regeneration system did not increase $q$. The lower calcium sensitivity may be partially explained by the $Mg^{2+}$ affinity of CrP compared to PEP, causing $[Mg^{2+}]$ to increase from 0.6 mM to 0.9 mM in CrP/K solutions. We also tested for an effect of temperature by working at 20°C. For the LDH/PK regeneration system, we obtained $K = 8.39 \pm 1.27 \times 10^5\ \mathrm{M}^{-1}$ (pK 5.92, $n = 9$), $q = 0.95$; and for CrP/K, $K = 7.86 \pm 1.51 \times 10^5\ \mathrm{M}^{-1}$ (pK 5.90, $n = 9$) and $q = 1.01$, showing no pronounced increase in $q$ from a temperature reduction, but a small increase in $K$, which is insignificant at a 10% probability level. Force-pCa curves constructed for flash-frozen porcine preparations at 28°C yielded $K = 6.80 \pm 1.81 \times 10^5\ \mathrm{M}^{-1}$ (pK 5.83, $n = 9$) and $q = 1.08$ (Fig. 1 *A*), indicating that flash-freezing did not cause a significant change in calcium sensitivity of force development ($p > 0.5$), nor did it alter $q$ appreciably.

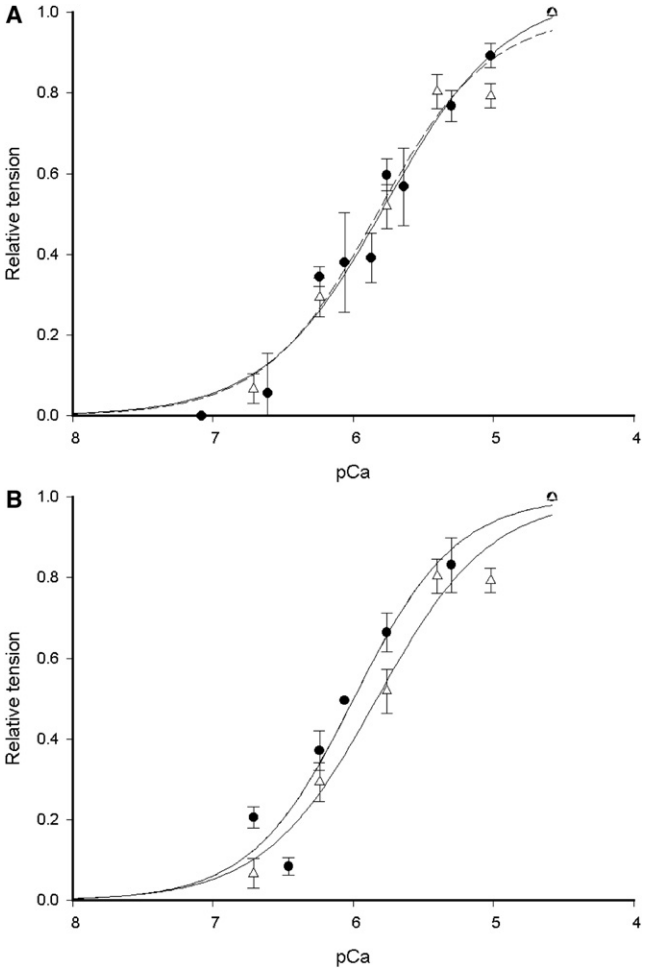


FIGURE 1 (*A*) Porcine force-pCa curves from 13 glycerinated (*solid symbols*) and 9 flash-frozen (*open symbols*) pieces of myocardium obtained at 28°C. Data points are the mean of relative tension developed averaged over all preparations. The fitted line of the Hill equation to the flash-frozen data is dashed to distinguish it from the continuous line of the glycerinated preparations. (*B*) Human force-pCa curve obtained from the average force development of 12 flash-frozen preparations (*solid symbols*) compared with 9 flash-frozen porcine samples (*open symbols*) obtained at 28°C.

$P_o$ (pCa 4.6) varied among preparations (6–49 kN $m^{-2}$, $n = 26$), with a mean of $24.74 \pm 3.55$ kN $m^{-2}$ for glycerinated myocardium and $15.77 \pm 3.70$ kN $m^{-2}$ (n = 9) for flash-frozen myocardium ($p = 0.058$). We also compared dynamic stiffness (i.e., the instantaneous force response to a length change; see section S.6 in the Supporting Material,) in calcium-activated and relaxed states using length steps of 0.5–0.8% fiber length. Dynamic relaxed stiffness (Young's modulus) was $974 \pm 158$ kN $m^{-2}$ for glycerinated ($n = 16$) and $577 \pm 59$ kN $m^{-2}$ for flash-frozen myocardium ($n = 9$),

$p = 0.025$. $Ca^{2+}$-activated stiffness was 1722 ± 256 kN $m^{-2}$ for glycerinated and 1050 ± 129 kN $m^{-2}$ for flash-frozen preparations, $p = 0.024$. Stiffness from four glycerinated preparations from the same heart as the flash-frozen samples was 476 ± 139 kN $m^{-2}$ in the relaxed samples, and 830 ± 47 kN $m^{-2}$ at 100% activation, and $P_o$ was 14.32 ± 1.97 kN $m^{-2}$. The similarity of this sample to the stiffness and $P_o$ of flash-frozen tissue suggests that the differences between glycerinated and flash-frozen tissue resulted from considerable intrinsic variability among hearts, although our data taken as a whole suggest a possible impairment of force transmission in flash-frozen tissue.

ATPase activity was calculated from NADH consumption at maximum activation. Maximum activity was 183 ± 27 $\mu$M $s^{-1}$ for glycerinated ($n = 16$) and 207 ± 41 $\mu$M $s^{-1}$ for flash-frozen myocardium ($n = 6$), an insignificant difference of 24 $\mu$M $s^{-1}$ ($p = 0.321$). Relaxed ATPase activity was 48 ± 7 $\mu$M $s^{-1}$ for glycerinated and 64 ± 8 $\mu$M $s^{-1}$ for flash-frozen samples. No reduction in this resting ATPase was achieved by addition of 500 $\mu$M ouabain ($n = 1$) and 10 mM azide ($n = 2$), whereas it was reduced by 11.3% using 400 $\mu$M cyclopiazonic acid ($n = 1$) and by 14.3% using 20 $\mu$M thapsigargin ($n = 3$); it is therefore unlikely that sodium or calcium pump activity in residual membrane systems forms more than a small part of the resting ATPase. Concentrations of 10 mM and 30 mM 2,3-butanedione 2-monoxime (BDM) reduced resting ATPase activity in flash-frozen myocardium to 86 ± 8% and 56 ± 5% of control ($n = 5$), respectively. Thapsigargin also reduced maximum $Ca^{2+}$-activated ATPase by 5.1% ($n = 2$).

Since NADH fluorescence declines faster in relaxing than in calibrating solution (i.e., in the absence of the ATP regeneration enzymes; see Fig. 2), and since interruption of UV illumination did not slow the rate of resting fluorescence decline, relaxed NADH fluorescence decay cannot arise from bleaching. ATPase activity plotted as a function of tension development showed a linear relationship (Fig. 3 *A*) with a nonzero intercept on the ordinate at zero force, suggesting that the $Ca^{2+}$-activated actomyosin ATPase is superimposed on some additional NADH consumption. If this resting ATPase were present at the same magnitude in the activated state, it should be subtracted to obtain the true $Ca^{2+}$-sensitive ATPase activity, giving 135 ± 23 $\mu$M $s^{-1}$ for glycerinated and 143 ± 40 $\mu$M $s^{-1}$ for flash-frozen tissue. All the parameters determined for cryopreserved and glycerinated porcine tissue are summarized in Table 1.

We reduced the enzyme units from 500 to 250 U/ml and found that ATPase activity was unchanged, showing that enzyme insufficiency is not rate-limiting in fluorescence decay. In addition, for four glycerinated porcine preparations, we measured ATPase activities in situ and also using a cuvette assay (section S.2 in the Supporting Material). Because of the much larger volume of the cuvette compared to the preparation, more enzyme is available for the linked assay, and therefore enzyme activity cannot be limiting.

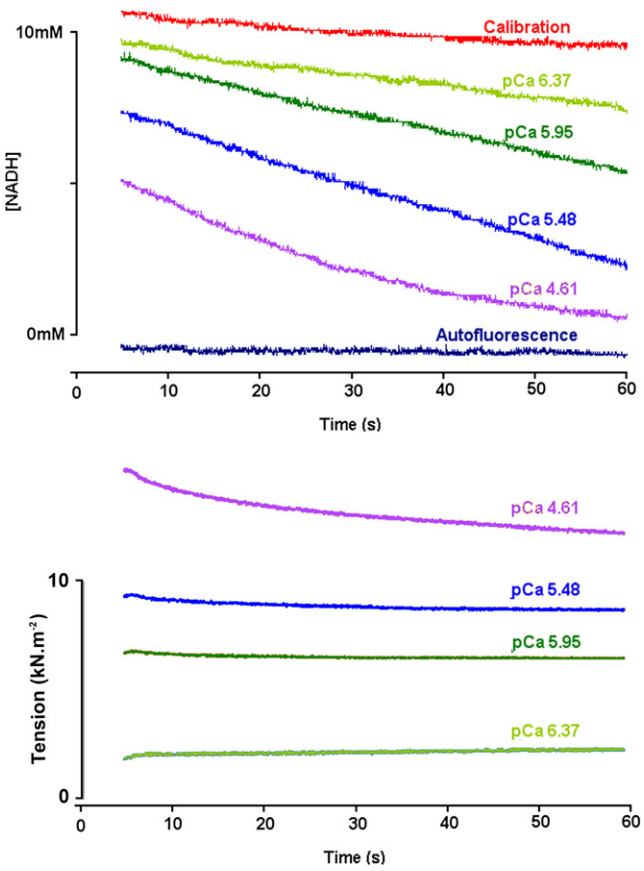


FIGURE 2 ATPase activity (measured as NADH fluorescence decline) (*upper*) and tension (*lower*) measured in a glycerinated porcine sample. The autofluorescence and the calibrating NADH fluorescence signal are also shown. At the lowest pCa value, the rate of NADH fluorescence decline shows flattening toward the end of the measurement due to NADH depletion. Bundle diameter, 425 $\mu$m. Temperature, 20°C.

NADH consumption in the cuvette was scaled to the NADH consumption rate in the tissue using the ratio of chamber to preparation volume. In these preparations, ATPase activity from the fiber assay was 129 ± 21 $\mu$M $s^{-1}$ and from the cuvette assay 112 ± 29 $\mu$M $s^{-1}$, suggesting that enzyme insufficiency did not affect ATPase activity measurements.

## Human myocardium

Calcium sensitivity of flash-frozen human myocardium was $K = 9.86 \pm 2.43 \times 10^5$ $M^{-1}$ (pK 5.99, $n = 12$) and $q = 1.18$. Fig. 1 *B* shows that both human and porcine force-pCa curves obtained from cryopreserved tissue are clearly similar, although the human curve is shifted 0.16 pCa units, a statistically insignificant difference from both cryopreserved ($p = 0.356$) and glycerinated porcine tissue ($p = 0.200$). $P_o$ was 16.77 ± 2.38 kN $m^{-2}$, insignificantly different from that of flash-frozen porcine ($p = 0.427$) but significantly different from that of glycerinated porcine tissue ($p = 0.039$) at a 5% level, and similar to the value of 18.6 kN $m^{-2}$ at 20°C reported by Narolska et al. (12) for similar-sized bundles of human myocytes. Dynamic

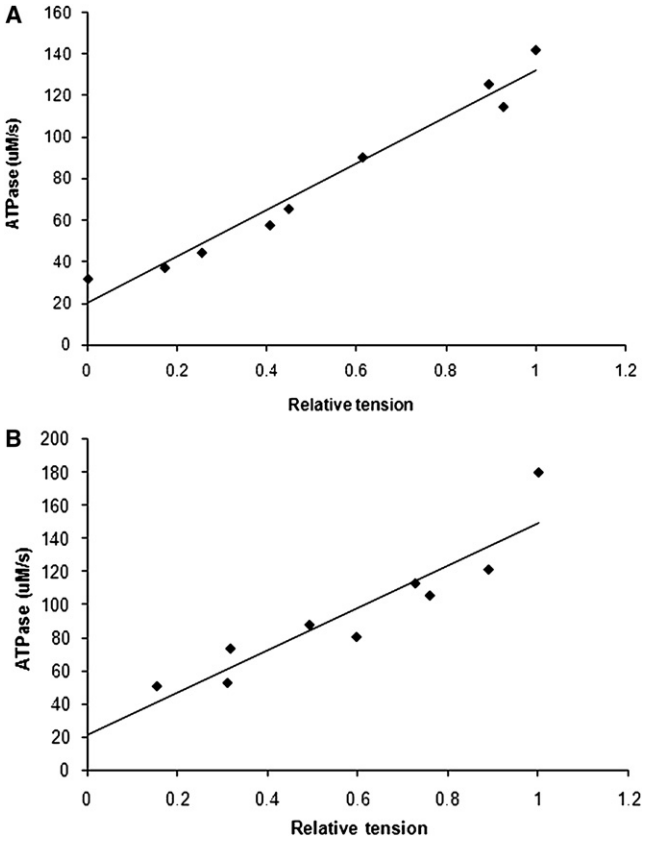


FIGURE 3 Slope of the NADH fluorescence time dependence has been converted into the rate of ADP production and is plotted as a function of isometric tension for the glycerinated porcine myocardium of Fig. 2 (*A*) and a flash-frozen human myocardium preparation (*B*). In both tissues, ATPase activity increases linearly with force (continuous line is a linear regression best fit), but the relation does not pass through the origin due to a residual ATPase activity in the relaxed state.

resting stiffness was 572 ± 92 kN m$^{-2}$ ($n = 26, p = 0.487$ and 0.011 against porcine myocardium flash-frozen and glycerinated, respectively), rising to 1178 ± 198 kN m$^{-2}$ ($p = 0.358$ and 0.054 against porcine flash-frozen and glycerinated, respectively) at maximum activation. Maximum ATPase activity in human myocardium was 132 ± 18 $\mu$M s$^{-1}$ (relaxed ATPase 41 ± 8 $\mu$M s$^{-1}$; Fig. 3 *B* and Fig. S2). This value significantly differs from the corresponding value for porcine tissue at a 10% level ($p = 0.055$ and 0.047 for glycerinated and flash-frozen porcine tissue, respectively). The mean increase in ATPase activity on full activation was therefore 91 ± 12 $\mu$M s$^{-1}$. Human myocardium mechanical parameters were smaller than those determined for glycerinated porcine muscle. In relaxed myocardium, tension and stiffness are determined by passive elastic elements composed of titin and collagen. Flash-freezing-induced damage to passive elasticity should be apparent in the passive tension dependence on sarcomere length. Fig. 4 *A* shows passive tension from 10 glycerinated porcine and 3 human myocardium samples at pCa 9 versus sarcomere length ($s$). Lines show the fitted function $as^k$. The similarity of the curves ($k = 5.15 \pm 0.62$ and $a = 0.13 \pm 0.08$ mN $\mu$m$^{-k}$ for porcine; and $k = 4.91 \pm 0.45$ and $a = 0.15 \pm 0.07$ mN $\mu$m$^{-k}$ for human myocardial tissue) suggests that passive elasticity is present in both with similar length dependence and in similar abundance in both tissues. Cross-bridge formation increases the total myocardial stiffness because of additional parallel elasticity within the cross-bridge linkages. If passive and cross-bridge elastic elements are present in approximately constant proportions in the sarcomere, the passive/cross-bridge dynamic stiffness ratio should also be constant. If cryopreservation reduced cross-bridge stiffness or damaged passive compliance, this ratio should be altered. We calculated this stiffness ratio as a function of sarcomere length for 12 glycerinated and 5 flash-frozen porcine preparations and 3 human myocardium samples (Fig. 4 *B*). The ratio increases at long sarcomere lengths, because cross-bridge stiffness falls and passive stiffness increases at reduced filament overlap. We chose rigor as the cross-bridge bound state to avoid effects of the sarcomere length on force and calcium ion affinity of the regulatory proteins, which are present in the $Ca^{2+}$-activated state. All three types of preparation showed similar stiffness ratios and sarcomere length dependency, suggesting that cryopreservation did not alter the relative amounts of passive and cross-bridge elastic elements in the tissues.

## Myofilament lattice effects on ATPase measurements

The linked assay system requires that substrate diffusion is sufficient to keep pace with ATP consumption. We monitored

**TABLE 1 Parameters for cryopreserved and glycerinated porcine and human myocardium**

| Parameters | Porcine (glycerinated) | Porcine (cryopreserved) | Human (cryopreserved) |
|---|---|---|---|
| $P_o$ (kN m$^{-2}$) | 24.74 ± 3.55 (16) | 15.77 ± 3.70* (6) | 16.77 ± 2.38$^{\dagger}$ (26) |
| Relaxed stiffness (kN m$^{-2}$) | 974 ± 158 (16) | 577 ± 59$^{\dagger}$ (6) | 572 ± 92$^{\dagger}$ (26) |
| Activated stiffness (kN m$^{-2}$) | 1722 ± 256 (16) | 1050 ± 129$^{\dagger}$ (6) | 1178 ± 198* (26) |
| Resting ATPase activity ($\mu$M s$^{-1}$) | 48 ± 7 (16) | 64 ± 8 (6) | 41 ± 8 (26) |
| Maximum ATPase activity ($\mu$M s$^{-1}$) | 183 ± 27 (16) | 207 ± 41 (6) | 132 ± 18* (26) |
| $Ca^{2+}$-sensitive ATPase activity ($\mu$M s$^{-1}$) | 135 ± 23 (16) | 143 ± 40 (6) | 91 ± 12$^{\dagger}$ (26) |
| $K$ (M$^{-1}$) | 5.87 ± 1.29 × 10$^5$ (12) | 6.80 ± 1.81 × 10$^5$ (9) | 9.86 ± 2.43 × 10$^5$ (17) |
| $q$ | 1.02 (12) | 1.08 (9) | 1.18 (17) |

Numbers in parentheses are $n$ values. Calcium sensitivity parameters were obtained from fits to pooled data from all preparations.
*Significantly different from glycerinated porcine at $p = 0.10$.
$^{\dagger}$Significantly different from glycerinated porcine at $p = 0.05$.

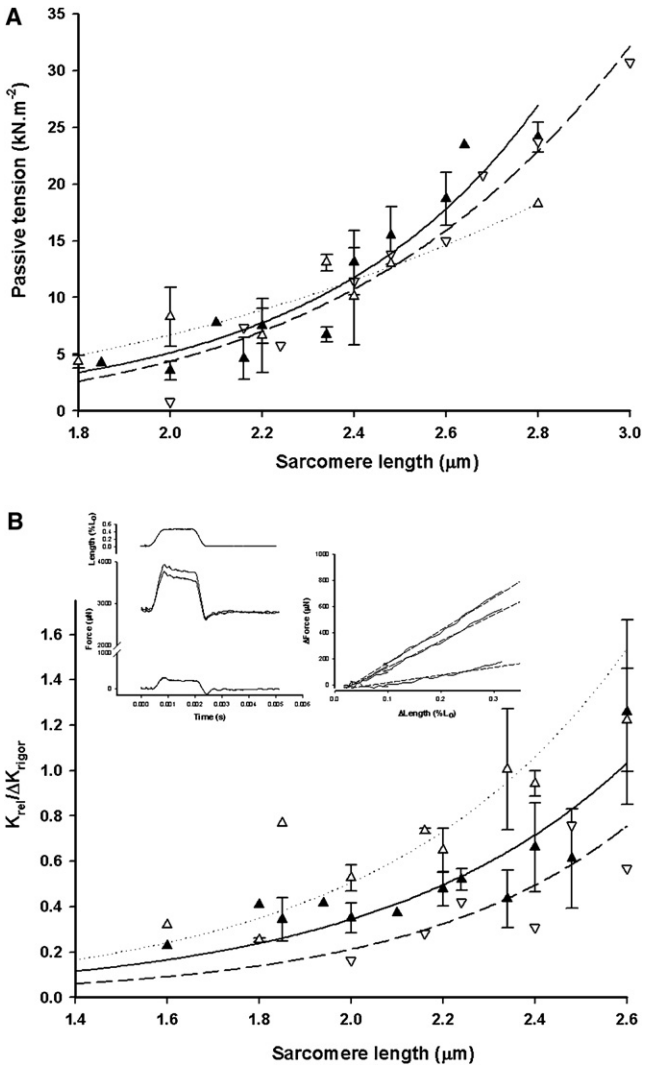


FIGURE 4 (*A*) Passive tension and (*B*) passive (relaxed) to rigor stiffness ratio plotted against sarcomere length. Glycerinated (*solid triangles*) and flash-frozen (*open triangles*) porcine data are plotted with standard errors, whereas flash-frozen human myocardium data (*inverted open triangles*) are plotted as individual data points. For *A*, the similarity between glycerinated porcine and flash-frozen human myocardium passive tension dependence on sarcomere length is apparent. Lines are fits of $as^k$, where $s$ is sarcomere length; $k = 5.15 \pm 0.62$ and $a = 0.13 \pm 0.08$ mN $\mu$m$^{-k}$ for porcine myocardium (*solid line*); and $k = 4.91 \pm 0.45$ and $a = 0.15 \pm 0.07$ mN $\mu$m$^{-k}$ for human myocardium (*dashed line*). In *B*; although human myocardium data points are shifted ~0.1 mm to the right of glycerinated porcine, flash-frozen porcine myocardium (*open triangles*) points are shifted to the left, so the position of the curves cannot be associated with cryopreservation. (*Left inset*) Length change as a percentage of fiber length, $L_0$ (*upper trace*), and force responses in activating solution (pCa 4.6), rigor (*middle traces*), and relaxing solution (*lower trace*). In general, rigor tension was close to that of maximum activation, but decreased after any mechanical disturbance. The rigor response here is the slightly larger of the middle two traces. (*Right inset*) Force-extension plots for the stretch phase of the length change, where rigor is the steepest line and relaxed is the shallowest. Force immediately before the stretch has been subtracted. The slope of the line was obtained as a linear regression of force upon length (*dashed lines*) and was taken as the dynamic stiffness. Flash-frozen human myocardium, diameter 400–450$\mu$m.

the fluorescence increase during preparation loading in 10 mM NADH solution over intervals from 0.8 to 600 s (Fig. S3). We estimated the NADH radial diffusion coefficient ($D$) by curve fitting to these loading data (section S.3 in the Supporting Material). Fiber bundles were not perfectly cylindrical, so we used mean diameter to apply the cylindrical solution (Eq. S3) and maximum and minimum diameters when applying the rectangular solution (Eq. S4). We estimated the attenuation coefficient of light passing through glycerinated porcine heart as $5617 \pm 620\ m^{-1}$ (equivalent to 7.7 mM NADH, $\lambda = 365$ nm). Using this value for five human preparations and eight porcine, the mean cylindrical $D$ was $2.18 \pm 0.43 \times 10^{-10}\ m^2\ s^{-1}$ and the rectangular $D$ estimate was $2.90 \pm 0.57 \times 10^{-10}\ m^2\ s^{-1}$. Conservatively taking the lower value, the half-time for NADH loading of a 300-$\mu$m-diameter fiber bundle is 6.5 s at 28°C. Because of the size of the muscle sample (70–120 mg) required for a tissue attenuation measurement, we did not attempt detergent treatment, which may have lowered tissue absorbance by removal of residual myoglobin. Reduced tissue absorbance would increase fluorescence from the center of the sample and increase radial diffusion coefficient estimates, so the values above may be slightly underestimated.

Disruption of cell membranes causes swelling, lowering the density of myosin filaments in the tissue and reducing measured ATPase activity. Swelling can be determined from the spacing of the equatorial reflections in the x-ray pattern (Fig. S7), which depends on the myofilament lattice dimensions (section S.5 in the Supporting Material). For five glycerinated porcine cardiac muscle preparations, before Triton treatment at sarcomere length 2.2 $\mu$m, we observed a nearest-neighbor thick filament spacing of $46.8 \pm 0.4$ nm. In three porcine preparations after Triton treatment, spacing increased to $50.1 \pm 0.4$ nm, whereas for five human preparations after Triton, spacing was $49.3 \pm 0.5$nm. Millman reports that the mammalian intact myocardium spacing is 43 nm at 2.2 $\mu$m sarcomere length (23), so our values show a lattice volume increase of 15% compared to glycerinated tissue before skinning and 30% compared to intact spacing. ATPase activity measurements should therefore be increased by 15–30% to allow for this lattice swelling when considering in vivo ATP consumption rates. In two experiments with human myocardium, we added 4% dextran T500 to the assay solutions, which restores the original, intact cell lattice spacing by osmotic compression. We found that lattice compression did not affect the linear relation between force and ATPase activity, but slightly increased its slope (13.3%).

## DISCUSSION

Many intrinsic cardiomyopathies are directly correlated with mutations in proteins essential to the regulation or generation of tension (24–28). Mutations affecting regulation alter the force-pCa curve parameters; those affecting force generation

may change cross-bridge binding, kinetics, or the energetic efficiency of the tissue, detectable in force generation and in the ATP hydrolysis rate; those affecting myocardial elasticity change the stiffness. Once these parameters are established for healthy human cardiac tissue, one may discover which are changed in myectomy samples from cardiomyopathic hearts. However, since our myectomy samples are flash-frozen, we must first evaluate any consequences of cryopreservation for these parameters. Ice crystallization damage can be avoided either by flash-freezing and maintaining at very low temperature ($\leq$-80°C) or by first exchanging part of the tissue water for glycerol (glycerination) and subsequent storage at $-20$°C to $-25$°C. Although tissue ultrastructure is well maintained by vitrification of cardiac muscle (29), cryopreservation is less effective in preservation of structure and function in both venous (30) and cardiac tissue (31). We assessed the effects of cryopreservation by comparing parameters measured in porcine myocardium that had been either cryopreserved or glycerinated, a recognized preservation technique for both cardiac and skeletal muscle preparations, which avoids completely the complications of ice crystallization. Flash-frozen porcine tissue force-pCa curves gave $K$ and $q$ values insignificantly different from those for glycerinated porcine myocardium ($6.80 \times 10^5$ $M^{-1}$, pK 5.83; $q = 1.08$, compared to $5.87 \times 10^5$ $M^{-1}$, pK 5.77; $q = 1.02$), indicating that cryopreservation did not affect porcine $Ca^{2+}$ sensitivity. Likewise, both human and porcine cryopreserved tissue gave sarcomere patterns of similar quality to those seen in glycerinated porcine muscle, suggesting that sarcomeric structure and order were not disrupted by the freezing procedure (9).

Interaction of actin and myosin in striated muscles is regulated by the binding of $Ca^{2+}$ to troponin C. Because cardiac muscle troponin contains only one functional regulatory calcium binding site and may exhibit less cooperativity between regulatory and contractile proteins, its force-pCa curve is flatter, yielding a slope ($q$ in Eq. 4) of 2–3, compared with values of 4 or greater for skeletal muscle (32). Slope values reported here are clustered around unity, implying reduced cooperativity under our experimental conditions. Papp et al. (33) showed that at low pH (6.5) and 10 mM inorganic phosphate, $q$ was reduced from 2.99 (pH 7.2) to 1.00 in nonfailing human myocytes, indicating a $q$ sensitivity to the chemical environment. According to our experiments, our low $q$ values cannot be attributed to temperature, choice of ATP regeneration system, or [$Mg^{2+}$]. We also failed to find a correlation between $q$ values and tissue dimensions. However, we noted a shift in $Ca^{2+}$ sensitivity toward lower pCas over the course of an experiment, which, because force development was averaged over the whole experiment, might account for a force-pCa curve flatter than that prevailing at any isolated moment in an experiment. In addition, the pCa curves in Fig. 2 were obtained by averaging tensions obtained from different preparations which, taking into account any statistical variation in calcium affinity among samples, might also tend to flatten the mean slope of the force-pCa relation.

$Ca^{2+}$ sensitivity ($5.87 \times 10^5$ $M^{-1}$, pK 5.77 for glycerinated porcine tissue; and $9.86 \times 10^5$ $M^{-1}$ pK 5.99 for human tissue) was similar to that determined by others. Our porcine muscle pK concurs with those of Szczesna et al. (pK 5.67 (2)) and Schoffstall et al. (pK 5.92 (34)), but is smaller than found by Toyo-oka (pK 6.7 (35)). For human ventricular myocardium, Pagani et al. (36) observed a pK of ~5.9, Narolska et al. reported pK values of 5.48 (37) and 5.68 (12), Okafor et al. a value of 5.55 (8), and Papp et al. a value of 6.30 (33). The range of pK values reflects the different chemical conditions and sarcomere lengths used in the construction of the force-pCa curves, with long sarcomere lengths well known to cause a leftward shift in the pCa-force curve for both skeletal and cardiac muscle (38–41).

$P_o$ in our experiments was small compared to both skeletal muscle and isolated cardiac myocytes, but was consistent with the value of 7.8 kN $m^{-2}$ for porcine muscle strips (34), and 18.6 kN $m^{-2}$ (12) and 26.9 kN $m^{-2}$ (37) for human samples. These values must be compared with tensions of ~100 kN $m^{-2}$ developed by isolated human cardiac myofibrils. Because our strips of myocardium have been cut from bulk muscle, estimates of sample cross-sectional area may include regions of muscle lacking mechanical continuity along the whole length of the preparation. However, in skinned myocardial samples from small animals, where trabecular and papillary muscle preparations can be used whole or with minimum dissection, the $P_o$ is similar to that reported here (P. J. Griffiths, R. Pelc, and L. Carrier, unpublished observations) (42). Alternatively, the fractional tissue volume occupied by a force-bearing contractile apparatus may vary depending on the relative age and fitness of the donors and on the region of the ventricles from which the samples are obtained. We estimate the fractional volume of both human and porcine myocardium occupied by myofibrils to be ~40% (see section S.4 in the Supporting Material), so myofibrillar isometric tension in our samples should be 2.5-fold greater than that determined for the entire cross-sectional area.

$P_o$ was different in flash-frozen and glycerinated porcine cardiac trabeculae, whereas human myocardium gave isometric tensions similar to those of flash-frozen porcine. Similarly, human passive and active stiffness were less than in glycerinated porcine muscle (59% and 68%, respectively) but similar to flash-frozen porcine tissue (Fig. 5), suggesting that cryopreservation might impair the axial transmission of tension. The dependence of passive tension on sarcomere length in human and glycerinated porcine tissue is similar (Fig. 4 *A*) and in agreement with data from others (43–46). The ratio of the stiffness increase in rigor (assumed to result from cross-bridge formation) to passive dynamic stiffness was similar in human and both types of porcine preparations, suggesting that the respective force-bearing structures were present in similar proportions and exhibited similar

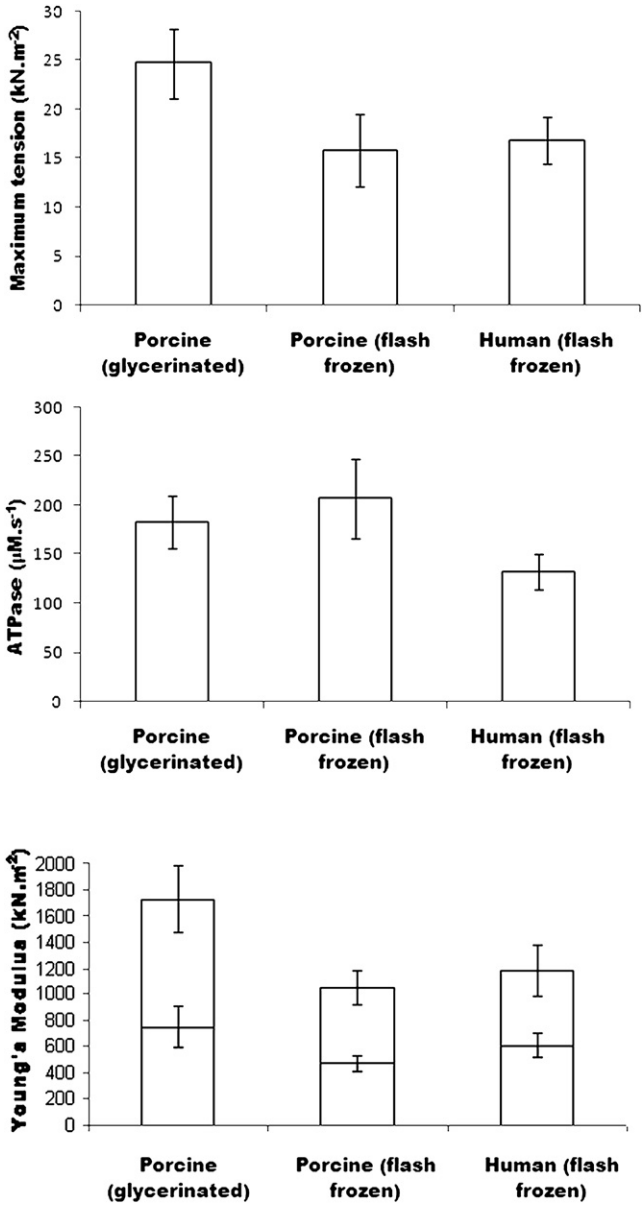


FIGURE 5 Data summary for maximum activated isometric tension (*upper*), maximum ATPase activity (*middle*), and passive and active dynamic stiffness (*lower*). The lower section of the columns represent passive and the upper part activated stiffness.

mechanical properties (Fig. 4 *B*, and see section S.6 in the Supporting Material). Likewise, direct comparison of flash-frozen and glycerinated porcine tissue from the same heart yielded similar mechanical parameters. In addition, $P_o$ in isolated human cardiac myofibrils from fresh and frozen tissue shows no impairment of tension generation as a result of freezing (47,48). Thus, although we cannot rule out an impairment of axial force transmission in flash-frozen tissue, our data might also be explicable by intrinsic variability among hearts with respect to fractional contractile tissue volume or by differing degrees of mechanical continuity, as discussed above.

Maximum ATPase activity in porcine myocardium, excluding that present in relaxing solution, was 135 $\mu$M s$^{-1}$ for glycerinated and 143 $\mu$M s$^{-1}$ for cryopreserved samples, whereas human tissue gave a much smaller activity, 91 $\mu$M s$^{-1}$, approximately twice the value obtained by Narolska et al. (12) for ventricular muscle at 20°C. Since ATPase activity was unaffected in our porcine samples, and since mechanical parameters were very similar in flash-frozen porcine and human myocardium, suggesting similar fractional volume occupancy, we conclude that ATPase activity is 33–36% lower in human than in porcine myocardium. ATPase activity in both human and porcine myocardia is considerably lower than in skeletal muscle (*Rana temporaria* sartorius, 435 ± 91 $\mu$M s$^{-1}$, $n = 12$ at 7°C; rabbit psoas, 306 ± 61 $\mu$M s$^{-1}$, $n = 8$ at 10°C), because both cardiac preparations contain principally slow isoforms of myosin, and in roughly similar proportions (49,50). Resting ATPase was relatively insensitive to SERCA inhibitors thapsigargin and cyclopiazonic acid, the sodium pump inhibitor ouabain, and the aerobic metabolic inhibitor sodium azide. BDM at a concentration of 30 mM suppressed resting ATPase activity by ~50%, suggesting that half the resting ATPase activity may be unregulated cross-bridge turnover, or that BDM dephosphorylated a phosphorylation-dependent kinase (51).

After Triton skinning, nearest-neighbor thick-filament spacing ($a$) was increased by 15–30%. The sarcomeric volume associated with a single thick filament is

$$\sqrt{3}/2a^2s,$$

where $s$ is the sarcomere length. The value in moles of S1 in this volume is $6l/14.34N$, taking 6 as the number of S1s per myosin crown, $N$ as Avogadro's number, $a$ as 50 nm, and $l$, the width of the A band, as 1600 nm, so that the concentration of S1 is ~0.23 mM (assuming the fractional volume occupied by the contractile apparatus to be 100%), giving a total maximum ATP turnover of 0.90–0.80 s$^{-1}$ for porcine and 0.57 s$^{-1}$ for human myocardium. This is in agreement with porcine ATP turnover measured by the cuvette assay technique at room temperature (0.48 s$^{-1}$ (11)), but is up to sixfold lower than corresponding values obtained from smaller species (52). The considerably higher heart rate in small animals may require a correspondingly higher myosin ATPase activity to drive contraction, whereas similar-sized species (pig and man) have similar ATP turnover rates.

The NADH diffusion coefficient in free solution in 0.1 M phosphate buffer, pH 7.4, at 20°C has recently been measured as $3.8 \times 10^{-10}$ m$^2$ s$^{-1}$ (53), though other values in the range 2.3–6.7 $\times$ $10^{-10}$ m$^2$ s$^{-1}$ have been reported under different experimental conditions. Our estimate of $D$ in skinned myocardium as $2.18 \times 10^{-10}$ m$^2$ s$^{-1}$ is only 57% of this value, probably because of the tortuosity of the diffusion path due to residual extracellular matrix and membrane systems, and to the myofilament lattice.

In summary, our findings show that glycerinated and cryopreserved porcine myocardia exhibit similar regulatory and biochemical properties, but mechanical properties differed. Human myocardium mechanical parameters resembled those of flash-frozen porcine myocardium. Differences in mechanical parameters among tissues may be attributed to consequences of the flash-freezing protocol, but more likely are due to variability in fractional volume occupied by the contractile apparatus or differences in the mechanical continuity of the myocardium. ATPase activity is insensitive to the flash-freezing protocol and to the mechanical continuity of the myocardium, and thus, differences between human and porcine cryopreserved myocardium indicate that ATP turnover is slower in human than in porcine tissue.

## SUPPORTING MATERIAL

Six sections, seven figures, and references are available at http://www.biophysj.org/biophysj/supplemental/S0006-3495(09)01368-X.

The authors thank Prof. S. M. Marston and Prof. C. dos Remedios for supplying human myectomy samples. We are indebted to Mr. Mohan Masih for his contribution to our ultrastructural studies.

This work was supported by the British Heart Foundation, the European Union, and DESY under Contract RII3-CT-2004-506008 (IA-SFS). R.P. was supported by Academy of Sciences grants LC06063 and AV0Z50110509.

## REFERENCES

1. Putkey, J. A., W. Liu, X. Lin, S. Ahmed, M. Zhang, et al. 1997. Fluorescent probes attached to cys-35 or cys-84 in cardiac troponin C are differentially sensitive to $Ca^{2+}$-dependent events *in vivo* and *in situ*. *Biochemistry*. 36:970–978.
2. Szczesna, D., R. Zhang, J. Zhao, M. Jones, G. Guzman, et al. 2000. Altered regulation of cardiac muscle contraction by troponin T mutations that cause familial hypertrophic cardiomyopathy. *J. Biol. Chem.* 275:624–630.
3. Preston, L. C., H. Watkins, and C. S. Redwood. 2006. A revised method of troponin exchange in permeabilised cardiac trabeculae using vanadate: functional consequences of a HCM-causing mutation in troponin I. *J. Muscle Res. Cell Motil.* 27:585–590.
4. Mazur, P. 1970. Cryobiology: the freezing of biological systems. *Science*. 168:939–949.
5. Baicu, S., M. J. Taylor, Z. Chen, and Y. Rabin. 2008. Cryopreservation of carotid artery segments via vitrification subject to marginal thermal conditions: correlation of freezing visualization with functional recovery. *Cryobiology*. 57:1–8.
6. Rubinsky, B. 2003. Principles of low temperature cell preservation. *Heart Fail. Rev.* 8:277–284.
7. van der Velden, J., Z. Papp, R. Zaremba, N. M. Boontje, J. W. de Jong, et al. 2003. Increased $Ca^{2+}$-sensitivity of the contractile apparatus in end-stage human heart failure results from altered phosphorylation of contractile proteins. *Cardiovasc. Res.* 57:37–47.
8. Okafor, C., R. Liao, C. Perreault-Micale, X. Li, T. Ito, et al. 2003. Mg-ATPase and $Ca^{2+}$ activated myosin ATPase activity in ventricular myofibrils from non-failing and diseased human hearts: effect of calcium sensitising agents MCI-154, DPI 201–106, and caffeine. *Mol. Cell. Biochem.* 245:77–89.
9. Jweied, E. E., R. D. McKinney, L. A. Walker, I. Brodsky, A. S. Geha, et al. 2007. Depressed cardiac myofilament function in human diabetes mellitus. *Am. J. Physiol. Heart Circ. Physiol.* 289:H2478–H2483.
10. Klotz, C., M. C. Aumont, J. J. Leger, and B. Swynghedauw. 1975. Human cardiac myosin ATPase and light subunits. A comparative study. *Biochim. Biophys. Acta*. 386:461–469.
11. Kuhn, H. J., C. Bletz, and J. C. Rüegg. 1990. Stretch-induced increase in the $Ca^{2+}$ sensitivity of myofibrillar ATPase activity in skinned fibres from pig ventricles. *Pflugers Arch.* 415:741–746.
12. Narolska, N. A., R. B. van Loon, N. M. Boontje, R. Zaremba, S. Eiras Penas, et al. 2005. Myocardial contraction is 5-fold more economical in ventricular than in atrial human tissue. *Cardiovasc. Res.* 65:221–229.
13. Griffiths, P. J., K. Güth, H. J. Kuhn, and J. C. Rüegg. 1980. ATPase activity in rapidly activated skinned muscle fibres. *Pflugers Arch.* 387:167–173.
14. Stephenson, D. G., A. W. Stewart, and G. J. Wilson. 1989. Dissociation of force from myofibrillar ATPase and stiffness at short sarcomere lengths in rat and toad skeletal muscle. *J. Physiol.* 410:351–366.
15. Hilber, K., Y. B. Sun, and M. Irving. 2001. Effects of sarcomere length and temperature on the rate of ATP utilisation by rabbit psoas muscle fibres. *J. Physiol.* 531:771–780.
16. Messer, A. E., A. M. Jacques, and S. B. Marston. 2007. Troponin phosphorylation and regulatory function in human heart muscle: dephosphorylation of Ser23/24 on troponin I could account for the contractile defect in end-stage heart failure. *J. Mol. Cell. Cardiol.* 42:247–259.
17. Perrin, D. D., and I. G. Sayce. 1967. Computer calculations of equilibrium concentrations in mixtures of metal ions and complexing species. *Talanta*. 14:833–842.
18. Griffiths, P. J., and A. Jones. 1994. A simple device for transfer of single muscle fibres by rotation between 70 $\mu$l chambers while making optical measurements. *J. Physiol. (Lond.)*. 480:5P.
19. Hoskins, B. K., C. C. Ashley, R. Pelc, G. Rapp, and P. J. Griffiths. 1999. Time-resolved equatorial X-ray diffraction studies of skinned muscle fibres during stretch and release. *J. Mol. Biol.* 290:77–97.
20. Dobson, G. P., S. Hitchins, and W. E. Teague. 2002. Thermodynamics of the pyruvate kinase reaction and the reversal of glycolysis in heart and skeletal muscle. *J. Biol. Chem.* 277:27176–27182.
21. Press, W. H., B. P. Flannery, S. A. Teukolsky, and W. T. Vetterling. 1990. Numerical Recipes: The Art of Scientific Computing. Cambridge University Press, Cambridge, MA.
22. Kentish, J. C., and G. J. M. Stienen. 1994. Differential effects of length on maximum force production and myofibrillar ATPase activity in rat skinned cardiac muscle. *J. Physiol.* 475:175–184.
23. Millman, B. M. 1998. The filament lattice of striated muscle. *Physiol. Rev.* 78:359–391.
24. Geisterfer-Lowrance, A. A. T., S. Kass, G. Tanigawa, H.-P. Vosberg, W. J. McKenna, et al. 1990. A molecular basis for familial hypertrophic cardiomyopathy: a $\beta$ cardiac myosin heavy chain gene missense mutation. *Cell.* 62:999–1006.
25. Poetter, K., H. Jiang, S. Hassanzadeh, S. R. Master, A. Chang, et al. 1996. Mutations in either the essential or regulatory light chains of myosin are associated with a rare myopathy in human heart and skeletal muscle. *Nat. Genet.* 13:63–69.
26. Thierfelder, L., H. Watkins, C. MacRae, R. Lamas, W. McKenna, et al. 1994. $\alpha$-Tropomyosin and cardiac troponin T mutations cause familial hypertrophic cardiomyopathy: a disease of the sarcomere. *Cell.* 77:701–712.
27. Watkins, H., D. Conner, L. Thierfelder, J. A. Jarcho, C. MacRae, et al. 1995. Mutations in the cardiac myosin binding protein-C gene on chromosome 11 cause familial hypertrophic cardiomyopathy. *Nat. Genet.* 11:434–437.
28. Satoh, M., M. Takahashi, T. Sakamoto, M. Hiroe, F. Marumo, et al. 1999. Structural analysis of the titin gene in hypertrophic cardiomyopathy: identification of a novel disease gene. *Biochem. Biophys. Res. Commun.* 262:411–417.
29. Sabanay, I., T. Arad, S. Weiner, and B. Geiger. 1991. Study of vitrified, unstained frozen tissue sections by cryoimmunoelectron microscopy. *J. Cell Sci.* 100:227–236.

30. Song, Y. C., B. S. Khirabadi, F. Lightfoot, K. G. M. Brockbank, and M. J. Taylor. 2000. Vitreous cryopreservation maintains the function of vascular grafts. *Nat. Biotechnol.* 18:296–299.

31. Schenke-Layland, K., J. S. Xie, S. Heydarkhan-Hagvall, S. F. Hamm-Alvarez, U. A. Stock, et al. 2007. Optimized preservation of extracellular matrix in cardiac tissues: implications for long-term graft durability. *Ann. Thorac. Surg.* 83:1641–1650.

32. Godt, R. E., and T. M. Nosek. 1989. Changes in intracellular milieu with fatigue or hypoxia depress contraction of skinned rabbit skeletal and cardiac muscle. *J. Physiol.* 412:155–180.

33. Papp, Z., J. van der Velden, A. Borbely, I. Edes, and G. J. Stienen. 2004. Effects of $Ca^{2+}$-sensitizers in permeabilized cardiac myocytes from donor and end-stage failing human hearts. *J. Muscle Res. Cell Motil.* 25:219–224.

34. Schoffstall, B., A. Clark, and P. B. Chase. 2006. Positive inotropic effects of low dATP/ATP ratios on mechanics and kinetics of porcine cardiac muscle. *Biophys. J.* 91:2216–2226.

35. Toyo-oka, T. 1981. Calcium ion-insensitive contraction of glycerinated porcine cardiac muscle fibers by Mg-inosine triphosphate. ITP as a tool to dissociate the contraction mechanism from the regulatory mechanism. *Circ. Res.* 49:1350–1355.

36. Pagani, E. D., R. Shemin, and F. J. Julian. 1986. Tension-pCa relations of saponin-skinned rabbit and human heart muscle. *J. Mol. Cell. Cardiol.* 18:55–66.

37. Narolska, N. A., N. Piroddi, A. Belus, N. M. Boontje, B. Scellini, et al. 2006. Impaired diastolic function after exchange of endogenous troponin I with C-terminal truncated troponin I in human cardiac muscle. *Circ. Res.* 99:1012–1020.

38. Endo, M. 1972. Stretch-induced increase in activation of skinned muscle fibres by calcium. *Nat. New Biol.* 237:211–213.

39. Hibberd, M. G., and B. R. Jewell. 1982. Calcium- and length-dependent force production in rat ventricular muscle. *J. Physiol.* 329:527–540.

40. Hofmann, P. A., and F. Fuchs. 1988. Bound calcium and force development in skinned cardiac muscle bundles: effect of sarcomere length. *J. Mol. Cell. Cardiol.* 20:667–677.

41. Cazorla, O., G. Vassort, D. Garnier, and J.-Y. le Guennec. 1999. Length modulation of active force in rat cardiac myocytes: is titin the sensor? *J. Mol. Cell. Cardiol.* 31:1215–1227.

42. Palmer, B. M., B. K. McConnell, G. H. Li, C. E. Seidman, J. G. Seidman, et al. 2004. Reduced cross-bridge dependent stiffness of skinned myocardium from mice lacking cardiac myosin binding protein-C. *Mol. Cell. Biochem.* 263:73–80.

43. Weiwad, W. K., W. A. Linke, and M. H. Wussling. 2000. Sarcomere length-tension relationship of rat cardiac myocytes at lengths greater than optimum. *J. Mol. Cell. Cardiol.* 32:247–259.

44. Nagueh, S. F., G. Shah, Y. Wu, G. Torre-Amione, N. M. King, et al. 2004. Altered titin expression, myocardial stiffness, and left ventricular function in patients with dilated cardiomyopathy. *Circulation.* 110: 155–162.

45. Makarenko, I., C. A. Opitz, M. C. Leake, C. Neagoe, M. Kulke, et al. 2004. Passive stiffness changes caused by upregulation of compliant titin isoforms in human dilated cardiomyopathy hearts. *Circ. Res.* 95:708–716.

46. Krűger, M., and W. A. Linke. 2006. Protein kinase-A phosphorylates titin in human heart muscle and reduces myofibrillar passive tension. *J. Muscle Res. Cell Motil.* 27:435–444.

47. Belus, A., N. Piroddi, B. Scellini, C. Tesi, G. D. Amati, et al. 2008. The familial hypertrophic cardiomyopathy-associated myosin mutation R403Q accelerates tension generation and relaxation of human cardiac myofibrils. *J. Physiol.* 586:3639–3644.

48. Piroddi, N., A. Belus, B. Scellini, C. Tesi, G. Giunti, et al. 2007. Tension generation and relaxation in single myofibrils from human atrial and ventricular myocardium. *Pflugers Arch.* 454:63–73.

49. Stelzer, J. E., H. S. Norman, P. P. Chen, J. R. Patel, and R. L. Moss. 2008. Transmural variation in myosin heavy chain isoform expression modulates the timing of myocardial force generation in porcine left ventricle. *J. Physiol.* In press.

50. Narolska, N. A., S. Eiras, R. B. van Loon, N. M. Boontje, R. Zaremba, et al. 2005. Myosin heavy chain composition and the economy of contraction in healthy and diseased human myocardium. *J. Muscle Res. Cell Motil.* 26:39–48.

51. Venema, R. C., R. L. Raynor, T. A. J. Noland, and J. F. Kuo. 1993. Role of protein kinase C in the phosphorylation of cardiac myosin light chain 2. *Biochem. J.* 294:401–406.

52. Ebus, J. P., and G. J. Stienen. 1996. ATPase activity and force production in skinned rat cardiac muscle under isometric and dynamic conditions. *J. Mol. Cell. Cardiol.* 28:1747–1757.

53. Banks, C. E., and R. G. Compton. 2005. Exploring the electrocatalytic sites of carbon nanotubes for NADH detection: an edge plane pyrolytic graphite electrode study. *Analyst (Lond.).* 130:1232–1239.